

SUPPLEMENTARY INFORMATION

Preparation of Single-Phase Three-Component Alkaline Earth Oxide of (BaSrMg)O: High Capacity and Thermally Stable Chemisorbent for Oxygen Separation

Xuncaï Chen,^a Taesung Jung,^b Jongho Park,^{*b} Woo-Sik Kim^{*a}

^a Department of Chemical Engineering, ILRI, Kyung Hee University, Yoing Kiheung-ku Seochun-dong, Kyungki-do 449-701, Republic of Korea

^b Korea Institute of Energy Research, 71-2, Jangdong, Yuseong-gu, Daejeon, Republic of Korea

Table S1. Element analysis of (BaSrMg)CO₃ crystal in different positions using EDS: cross-section and surface.

position	At%		
	Mg	Ba	Sr
cross-section	41.97	52.00	6.03
surface	41.93	51.49	6.58

Table S2. Element analysis of (BaSr)CO₃ crystals using EDS and ICP.

Detector	At%	
	Ba	Sr
EDS	80.09	19.91
ICP	77.54	22.46

Table 3. Element analysis of (BaSrMg)CO₃ crystals synthesized at the different reactant concentration ratio of [Mg(NO₃)₂]/[(BaSr)CO₃] using EDS.

Reactant Concentration Ratio [Mg(NO ₃) ₂]:[(BaSr)CO ₃]	Product Crystals		
	At %		
	Ba	Sr	Mg
0.5	51.70	5.67	42.63
0.6	50.89	5.21	43.9
0.7	52.49	6.00	41.51
0.8	50.44	6.24	43.32
0.9	51.41	5.97	42.62
1.0	51.49	6.58	41.93

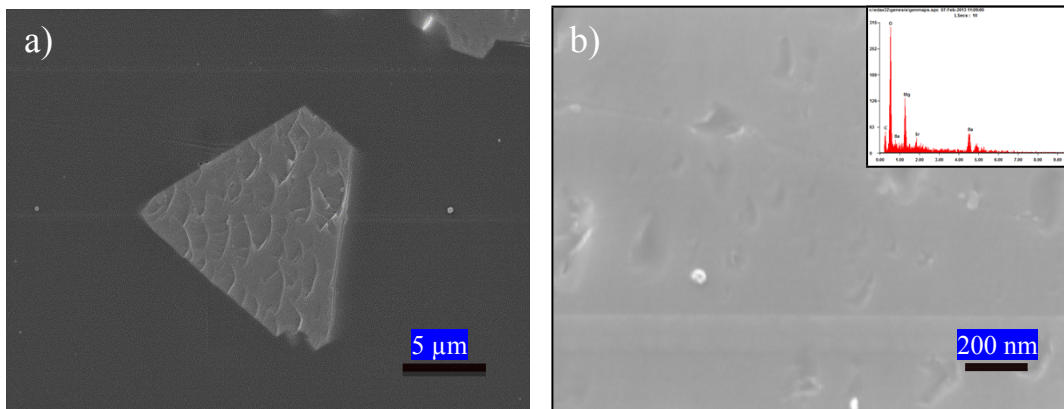


Figure S1. Analysis of (BaSrMg)CO₃ crystal cross-section by using FE-SEM and EDS.

(a) cross-sectional image of (BaSrMg)CO₃ crystal by FE-SEM, and (b) element analysis at cross-section of (BaSrMg)CO₃ crystal by EDS.

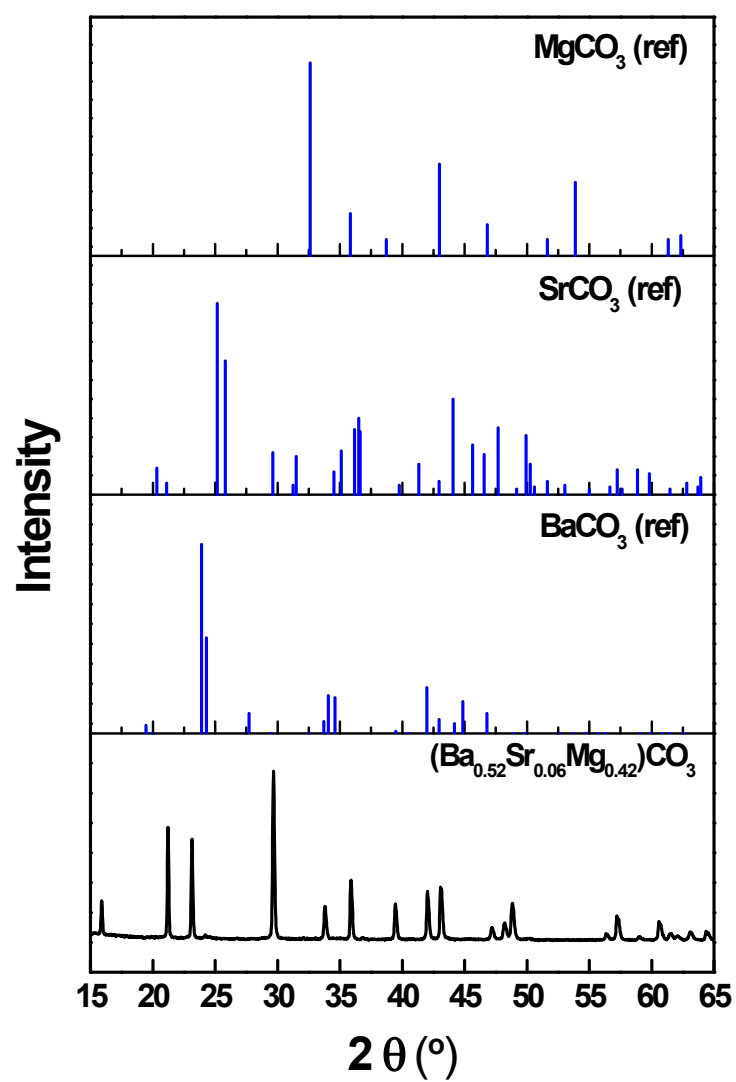


Figure S2. XRD pattern of (BaSrMg)CO₃ crystals comparing with JCPDS data of BaCO₃ (JCPDS number:05-0378), SrCO₃ (JCPDS number:05-0418), and MgCO₃ (JCPDS number:08-0479).

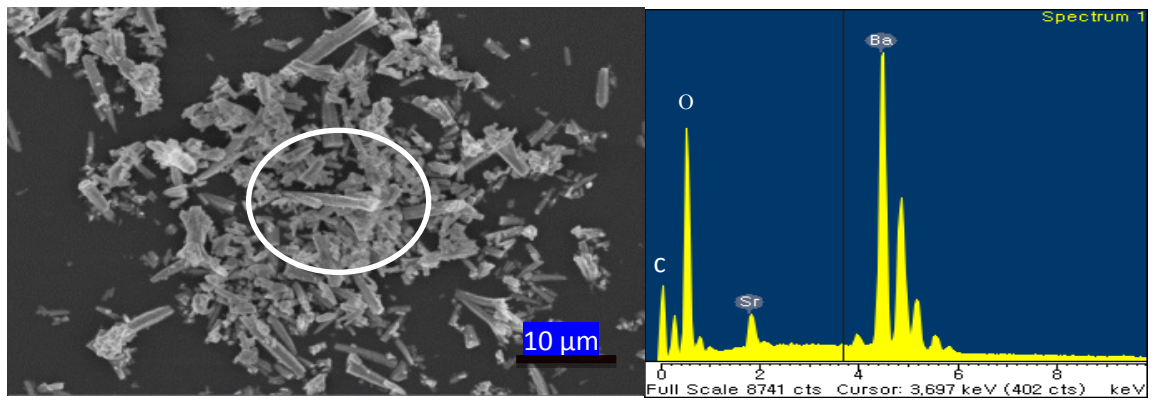


Figure S3. Analysis of $(\text{BaSr})\text{CO}_3$ crystals by FE-SEM and EDS.

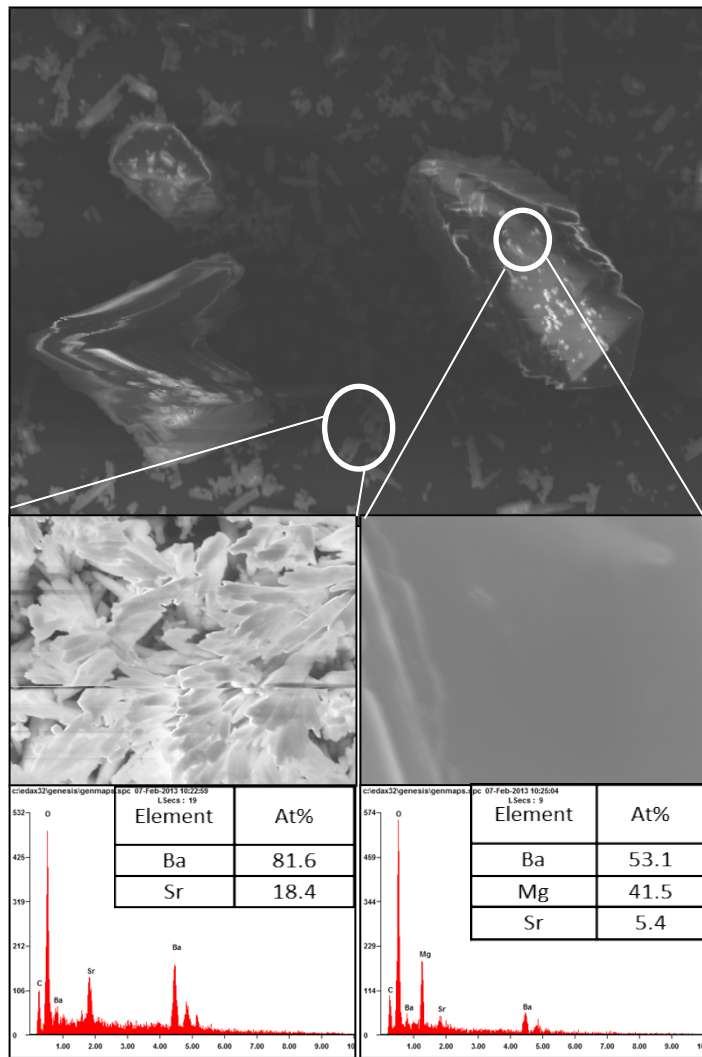


Figure S4. Analysis of solid mixture produced at reactant concentration ratio of $[\text{Mg}(\text{NO}_3)_2]/[(\text{BaSr})\text{CO}_3]=0.6$ by FE-SEM and EDS, (a) needle-shaped $(\text{BaSr})\text{CO}_3$ crystals and (b) hexagon-shaped $(\text{BaSrMg})\text{CO}_3$ crystals.

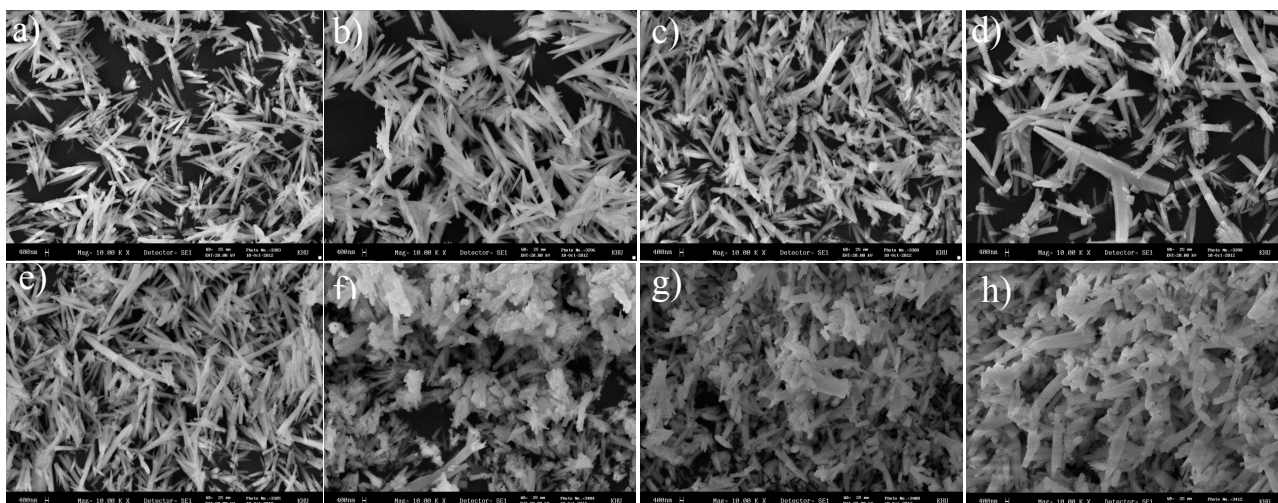


Figure S5. Effect of reactant concentration ratio, $[\text{Ba}(\text{NO}_3)_2]/[\text{Sr}(\text{NO}_3)_2]$, on coprecipitation of $(\text{BaSr})\text{CO}_3$. (a) reactant concentration ratio of 0.9:0.1, (b) reactant concentration ratio of 0.8:0.2, (c) reactant concentration ratio of 0.7:0.3, (d) reactant concentration ratio of 0.6:0.4, (e) reactant concentration ratio of 0.5:0.5, (f) reactant concentration ratio of 0.4:0.6, (g) reactant concentration ratio of 0.3:0.7, (h) reactant concentration ratio of 0.2:0.8.

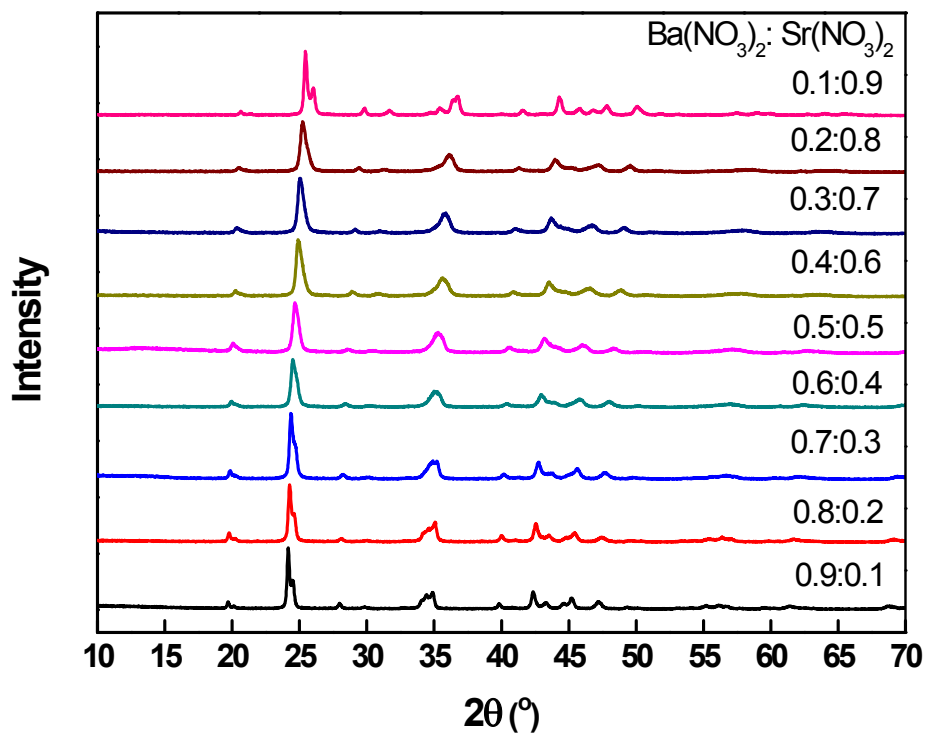


Figure S6. XRD patterns of (BaSr)CO₃ crystals synthesized at the different reactant concentration ratio of [Ba(NO₃)₂]/[Sr(NO₃)₂].

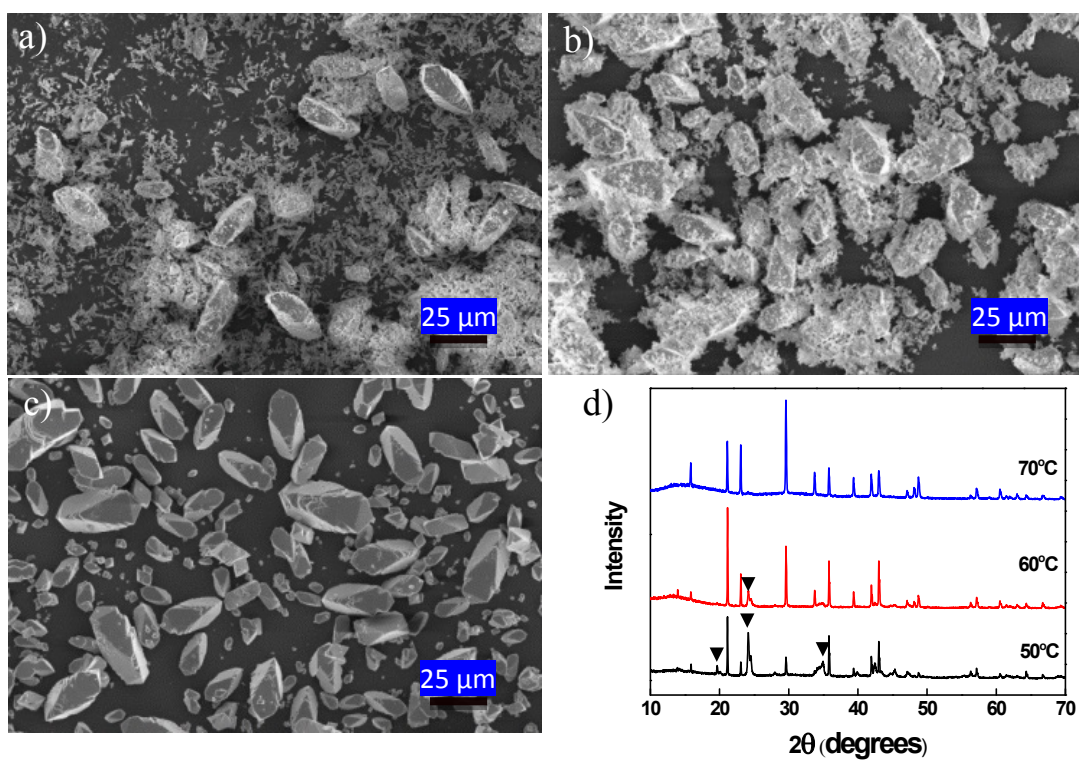


Figure S7. Effect of reactant temperature on co-precipitation of $(\text{BaSrMg})\text{CO}_3$ crystals. (a) 50 °C, (b) 60 °C, (c) 70 °C, (d) XRD patterns of product crystals.

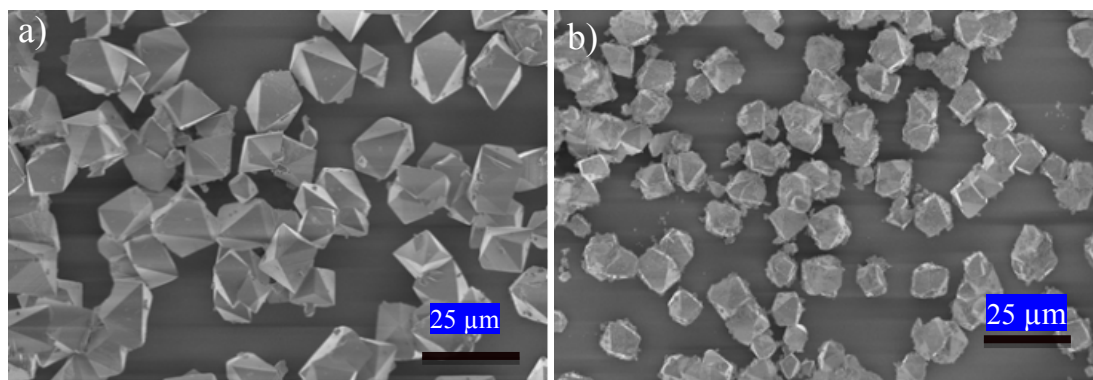


Figure S8. Effect of reactant concentration of $(\text{NH}_4)_2\text{CO}_3$ on co-precipitation of $(\text{BaSrMg})\text{CO}_3$ crystals. (a) 0.08 g/mL, (b) 0.12 g/mL.